A Dynamic Simulation Framework for Performance Analysis of a Three-Phase Separator

Michel Cardoso Natividade[1*], Reinaldo Coelho Mirre[2], Igor Oliveira de Freitas Campos[3]
[1]Chemical Engineering, – PRH 27.1 ANP/FINEP – Exploration, Development and Production of Oil, Natural Gas and Biogas; [2]Federal University of Bahia; [3]SENAI CIMATEC University; Salvador,Bahia, Brazil

The present study addresses the mathematical modeling and dynamic simulation of a three-phase gravitational separator. The overall goal was robust construction and modeling to optimize the reduction of water composition in crude oil emulsions. The presence of emulsified water severely impacts primary oil processing, decreasing the final quality of the product (increase in BS&W - Basic Sediment and Water), exponentially increasing operating costs (OPEX). For the construction of the model, the Python language was used, implementing mass balances and equations that describe the dynamics of phase separation. Correlations from the literature were incorporated for the calculation of fluid properties, such as density, and efficiency of the phases as a function of API gravity, and the classification of the oils used in the simulation scenarios themselves was validated. The results obtained show that the model was successful in describing the behavior of the system. Notably, the simulations demonstrated that oils with higher API gravity (lighter, with lower density) have faster and more efficient separation kinetics. This is because the lower viscosity of the oil (continuous phase) offers less resistance to the movement of water droplets, and the greater density difference between the phases intensifies the gravitational force, accelerating decantation. The behavior of the model compared to real scenarios can be correlated with the impact of the chemical composition, and the higher concentration of components such as asphaltenes and resins, natural emulsifiers present in oils, in heavy oils tend to form more rigid interfacial films, stabilizing the emulsion, making it difficult to coalescence. It is concluded that the simulated model obtained satisfactory accuracy, presenting results consistent with the theory and industrial practice in all the proposed scenarios, proving to be a valuable tool for the analysis and optimization of separation processes.
Keywords: Primary Petroleum Processing. Crude Oil. BS&W. Three-phase Separator. Mathematical Modeling.

Hydrocarbon production in fields such as pre-salt involves the extraction of a multiphase mixture of oil, gas, and water. The energy introduced into this flow during lifting, especially due to high pressure drops in valves and shear in pumps, disperses the water in the oil phase, creating emulsions that can be highly stable [1].

Emulsions are phenomena found in the primary processing of petroleum, caused by adverse factors, formed by the intense agitation (shearing) to which the fluids are subjected during the production and transport processes. Thus, some compounds found in crude oil aid in the formation of emulsions, such as asphaltenes and resins.

These emulsions can be formed into oil, water, gas, and solids, and are classified as oil-in-water, water-in-oil, depending on the predominant fluid in the phase. There are several techniques for the treatment of these emulsions, which derive from the emulsion content, cost, and development of the technology [2,3].

Demulsification can be performed using various techniques, the choice of which depends on factors such as emulsion characteristics, investment (CAPEX) and operational (OPEX) costs, the level of technological development, and other related variables. The goal of applying these technologies is to ensure that the treated oil meets the rigorous quality standards required for its commercialization.

In Brazil, oil commercialization is regulated by the National Petroleum Agency (ANP), which establishes specifications to ensure oil quality. Among these, the water and sediment content (BS&W) must be equal to or less than 1.0% by volume. Additionally, the ANP stipulates a limit for salt concentration, which must be a maximum of 285 mg/L [2-5].

Received on 16 December 2025; revised 15 February 2026.
Address for correspondence: Michel Cardoso Natividade. Av. Orlando Gomes, 1845, Piatã, Salvador, Bahia, Brazil. Zipcode: 41650-010. E-mail: michel.cardooso@fbest.org.br.

J Bioeng. Tech. Health 2026;9(3):237-246

With the excessive costs of CAPEX and OPEX in upstream oil industries, new layouts are sought that offer greater techno-economic efficiency. An essential tool for this purpose is process modeling, and consequently process simulation [6,7]. This work develops a dynamic simulation model in Python for a three-phase separator, with the objective of analyzing its operational performance for different API degrees, specifically in separation efficiency, as well as in the stability of interface levels.

Materials and Methods

The method for this work began with a literature review on water-oil separation methods and modeling approaches for BS&W reduction. The mathematical model was developed based on the formulation from Condori (2014) [5] for three-phase separators, representing an evolution of previous work by Natividade and colleagues (2024) [7], in which calculations for phase efficiency and mixture density were enhanced using experimental data and fluid properties supplemented by Filgueiras (2005) [6]. The model was implemented in Python and validated against results from the literature.

Finally, a case study was conducted to analyze the impact of different API gravities on the separator's performance. Figure 1 summarizes the steps of this method.

Figure 1. Method diagram in the applied research.

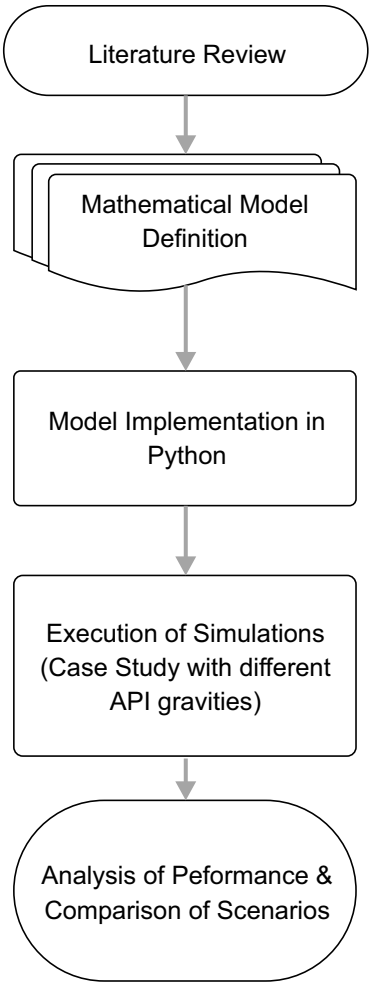

System Modeling

Three-Phase Separator

The three-phase separator is a cylindrical shaped equipment, which has some internal components making it help in the separation of phases, shown in the Figure 2.

The separator is designed to operate at low to medium pressures, such as temperatures above ambient. The vase consists of a few sections:

Separation Chamber

Upon entering the separation chamber, the multiphase flow loses momentum, initiating a separation process governed by gravity and the distinct densities of the fluids. The gas, being the least dense phase, immediately rises to occupy the upper vapor space of the vessel. Simultaneously, the liquid components stratify. Water, being denser, settles to the bottom, while the oil, with an intermediate density, forms a distinct layer on top of the water.

Secondary Separation Section

In this section, gas make up the largest volume of the section. As it has the phenomenon of dragging part of the liquid droplets, it is necessary to use mechanical devices such as mist eliminators.

Figure 2. Graphical diagram of a three-phase separator.

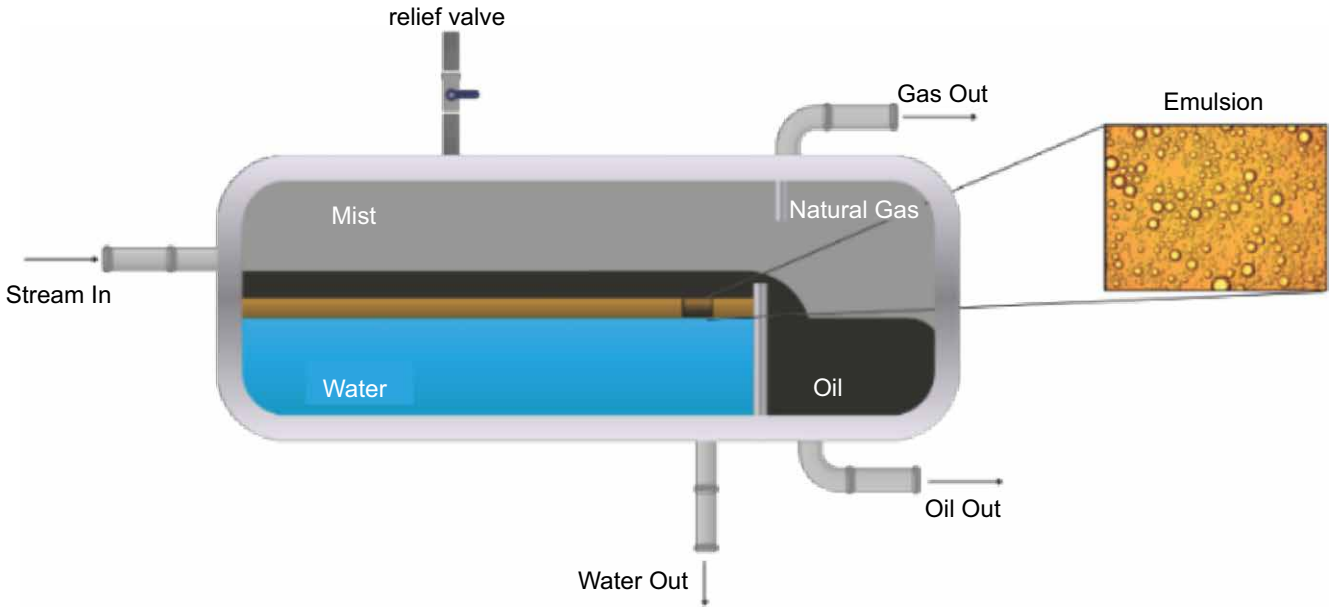

Source: Júnior (2023) adapted [8].

Oil Chamber

Phase separation in the vessel is achieved through gravitational settling, a process enhanced by inertial effects at the baffle plate and droplet coalescence. This separation occurs because of the density difference between the fluids.

As a result, the oil, being lighter, rises and accumulates in the upper part of the separation chamber. From there, it flows over a weir to a collection section located downstream of the baffle plate.

Inertial separation – sudden changes in velocity and flow direction allowing the gas to detach from the liquid phase due to the inertia that this phase has.

Agglutination of the particles – contact of the oil droplets dispersed on a surface, which facilitates its coalescence, agglutination, and consequent decantation [7].

The model developed in this work is based on the thesis by Condori (2014) [5], which proposes a simplified approach. The main simplifications adopted include disregarding interphase drag, treating the gas as ideal, and not modeling the droplet size distribution. This approach diverges from more rigorous methods, the importance of which for the thermodynamic representation of gases had already been highlighted by Nunes (1994) [9] showing that the thermodynamic representation of the phases is important in the study of gases, but has little significant effect on the dynamics of liquid/liquid separation, considering that there is no mass transfer between the thermodynamic phases. For the efficiencies of the aqueous and oily phases, Ribeiro (2016) [10] empirical constants were used, based on the Filgueiras (2005) model [6].

Balance Equations

The mathematical modeling in this work is based on the application of mass balances to three distinct control volumes: the separation chamber, the oil chamber, and the gas space. From these balances, the equations that describe the dynamic behavior of the system are derived, as well as the flow rates and properties of the separator's outlet streams.

Mass Balance in the Separation Chamber

The flow modeling in the separation chamber considers two distinct operational regimes, designated Case 1, and Case 2. The first case occurs when the height of the oil layer is less than the total emulsion height in the chamber, resulting in standard flow behavior. The second case, in turn, represents the condition where the oil height equals the total emulsion height, characterizing an overflow, which directly affects the phase separation efficiency. Each scenario results in a distinct set of equations to describe the flow, as illustrated in Figure 3 and Equations 1 to 7.

Figure 3. Systems generated inside the separator due to the presence of the baffle.

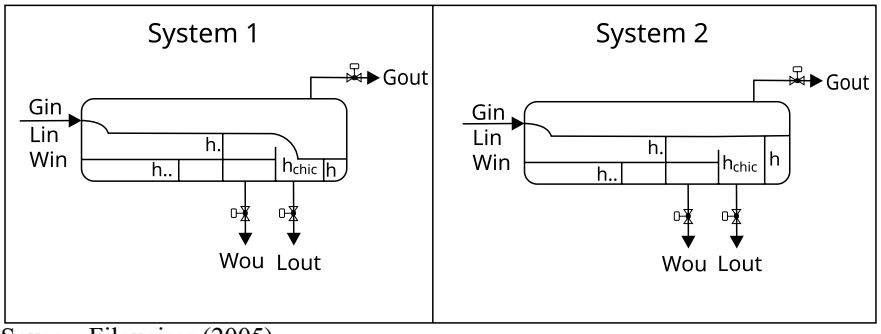

Source: Filgueiras (2005).

$$\frac{dh_{wy(t)}}{dt} = \frac{\{W_{ey} \cdot [1 - TOG_{ey} \cdot ef_{lwy}] + L_{ey} \cdot BSW_{ey} \cdot ef_{wly} - W_{sy}\}}{2 \cdot C_{Csy} \cdot \sqrt{h_{wy}[D_y - h_{wy}]}} \quad (1)$$

Case 1 ($\boldsymbol{h_{ty} < h_{vert}}$)

$$\frac{dh_{ly}(t)}{dt} = \frac{[L_{vy} - L_{Sy}]}{2 \cdot C_{cly}\sqrt{h_{ly} \cdot [D_y - h_{ly}]}} \quad (2)$$

$$\mathrm{L_{vy}} = 0 \quad (3)$$

$$\frac{\mathrm{dh_{ty}}(t)}{\mathrm{dt}} = \frac{1}{\mathrm{C_{csy}} \cdot \sqrt{h_{ty} \cdot (D - h_{ty})}} \cdot (\mathrm{W_e} + \mathrm{L_e} - \mathrm{L_{vy}} - \mathrm{W_{sy}}) \quad (4)$$

Case 2 ($h_{ty} > h_{vert}$)

$$\frac{dh_{ly}(t)}{dt} = \frac{dh_{ty(t)}}{dt} \quad (5)$$

$$\mathrm{L_{vy}} = \frac{\mathrm{k}}{60} \cdot (L_{vert} - 0.2 \cdot (h_{ty} - h_{vert}) \cdot (h_{ty} - h_{vert})^{1.5} \quad (6)$$

$$\frac{dh_{ty}(t)}{dt} = \frac{W_{ey} + L_{ey} - L_{sy} - W_{sy}}{\left(2 \cdot (C_{csy} + C_{cly}) \cdot \sqrt{h_{ty} \cdot (D - h_{ty})}\right)} \quad (7)$$

Output Equations of Separator Currents

$$G_{s(t)} = \frac{CV_{maxgy} \cdot S_{gy}}{\frac{2{,}832 \cdot 60 \cdot P_y \cdot MW_g}{R \cdot T_y}} \cdot \sqrt{\left(P_y + P_{comp_y}\right) \cdot \left(P_y - P_{comp_y}\right) \cdot d_g} \quad (8)$$

$$L_{sy} = \frac{CV_{maxly} \cdot S_{ly}}{0.0693 \cdot 60 \cdot \rho_{fl}} \cdot \sqrt{(P_y - P_{jusy}) \cdot d_l + \gamma_l \cdot h_{ly} \cdot 10^{-4}} \quad (9)$$

$$W_{sy} = \frac{CV_{maxwy} \cdot S_{wy}}{0.0693 \cdot 60 \cdot \rho_{fw}} \cdot \sqrt{(P_y - P_{jusy}) \cdot d_w + \{\gamma_w \cdot h_{wy} + \gamma_l \cdot [h_{ty} - h_{wy}]\} \cdot 10^{-4}} \quad (10)$$

$$\frac{dP_y(t)}{dt} = \frac{\{[W_{ey} + L_{ey} + G_{ey} - W_{sy} - L_{sy} - G_{sy}] \cdot P_y\}}{V_{ty} - V_{csy} - V_{cly}} \quad (11)$$

Results and Discussion

Initially, to perform a sensitivity analysis of how different oil compositions will behave in the separator, it is important to relate the types of oils. Farah [11] classify the main types of oils present, according to their API gravity, as evidenced in Table 1.

Table 1. Oil classification as of API gravity.

°API	Oil Classification
°API< 15	Asphaltic
15 < °API< 19	Extra Heavy
19 < °API< 27	Heavy
27 < °API< 33	Medium
33 < °API< 40	Light
40 < °API< 45	Extra Light

Numerical Solution

For the solution of the system of ordinary differential equations (EDOs) that describe how the three-phase separator behaves, the fourth order Runge-Kutta (RK4) was used. This method is widely used in engineering simulations due to its high accuracy and computational stability [13] The RK4 method makes it possible to bring the solution of an EDO closer to the $\frac{d\omega}{dt} = f(t, \omega)$ from an initial condition known as ωi in time ti. The subsequent value, $\omega i+1$, at a time $ti+1 = ti + h$ where h is the integration step, being calculated by the following Equation 12:

$$\omega_{i+1} = \omega_i + \frac{h}{6} \cdot (k_1 + 2 \cdot k_2 + 2 \cdot k_3 + k_4) \quad (12)$$

The coefficients k1-k4 represent slopes calculated at strategic points of the integration interval:

$$k_1 = hf(t, \omega) \quad (13)$$

$$k_2 = hf\left(t + \frac{h}{2}, \omega + \frac{k_1}{2}\right) \quad (14)$$

$$k_3 = hf\left(t + \frac{h}{2}, \omega + \frac{k_2}{2}\right) \quad (15)$$

$$k_4 = hf(t + h, \omega + k_3) \quad (16)$$

Numerical Simulation Results

Table 2 presents the values used for the initial conditions, input variables, and operational parameters of the model.

To evaluate the separator's performance across multiple scenarios, simulations were carried out using various API gravities (detailed in Table 1).

The dynamic model proved to be robust, as evidenced by the high stability of the operational pressure, which varied minimally (on the order of 0.1-0.2 kgf/cm²). Furthermore, the main performance result, illustrated in Figure 4, is that lighter oils (higher API gravity) achieve greater separation efficiency, leading to a lower BS&W content in the outlet stream.

As demonstrated in Figures 5 and 6, there is a direct correlation between the oil's API gravity and the separation efficiency, such that lighter oils (higher API gravity) result in higher flow rates at the separator's oil outlet.

From the scenarios evaluated, in different classifications of oils, as illustrated in Figure 7,

Table 2. Parameters of the three-phase separator.

$P = \frac{15kg}{cm^2}$	T = 305 K	$W_e = 0.184\frac{m^3}{h}$	$S_l = 0.5$
$M = 28.97g/mol$	$h_{ly} = 2.328m$	$L_e = 6.006e^{-3} \cdot \frac{m^3}{h}$	$S_g = 0.43638$
$\rho_{water} = \frac{965kg}{m^3}$	$h_{wy} = 1.152m$	$G_e = 7.182e^{-2}\frac{m^3}{h}$	$S_w = 0.79$
$\rho_{oil} = \frac{855kg}{m^3}$	$h_{ty} = 2.5171m$	BS&W = 0.02	$h_{vert} = 2.8m$

Figure 4. Pressure variation by BS&W out (%).

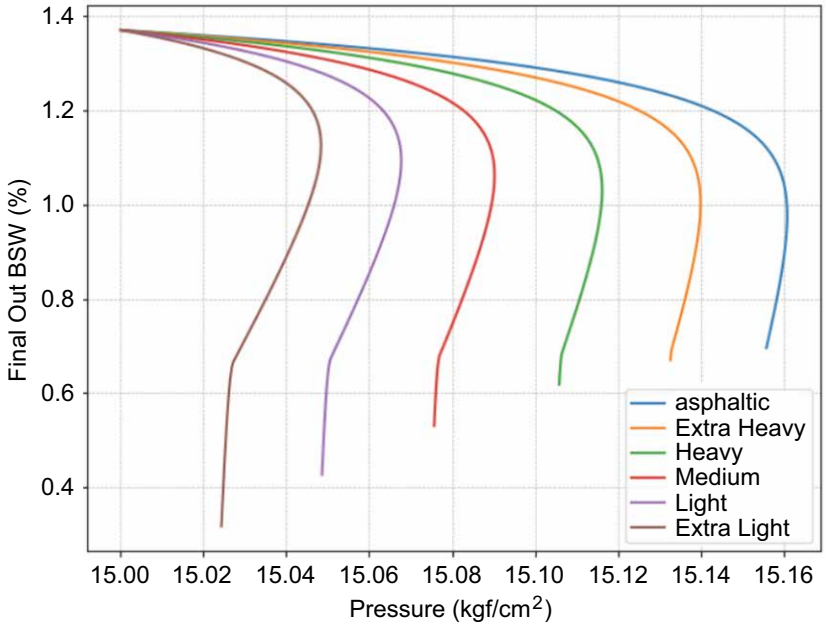

Figure 5. Oil outflow by oil gravity.

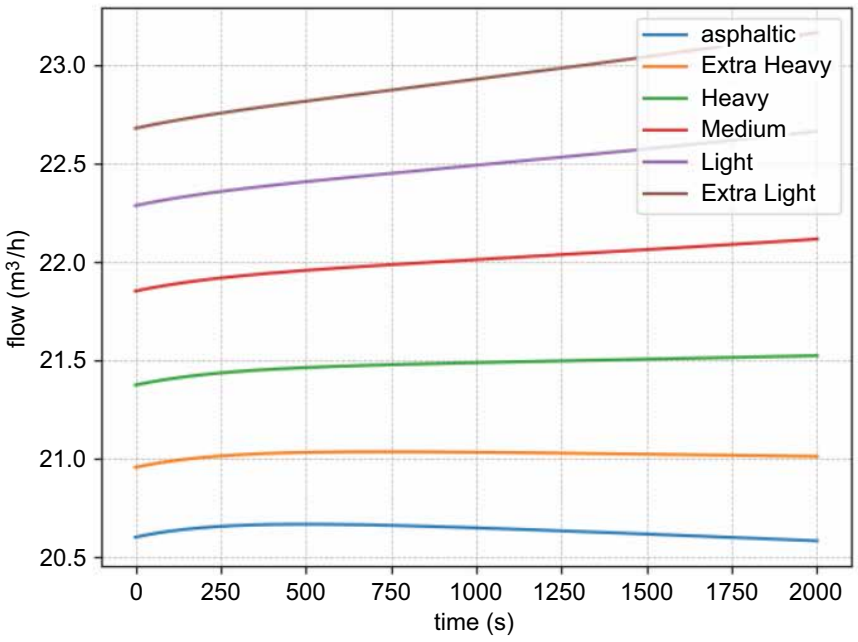

Figure 6. Pressure in separator by oil gravity.

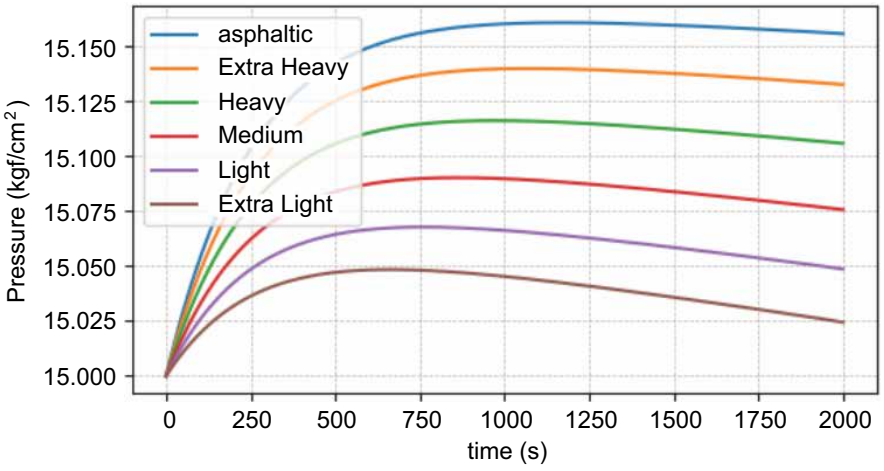

Figure 7. BS&W out oil by oil gravity.

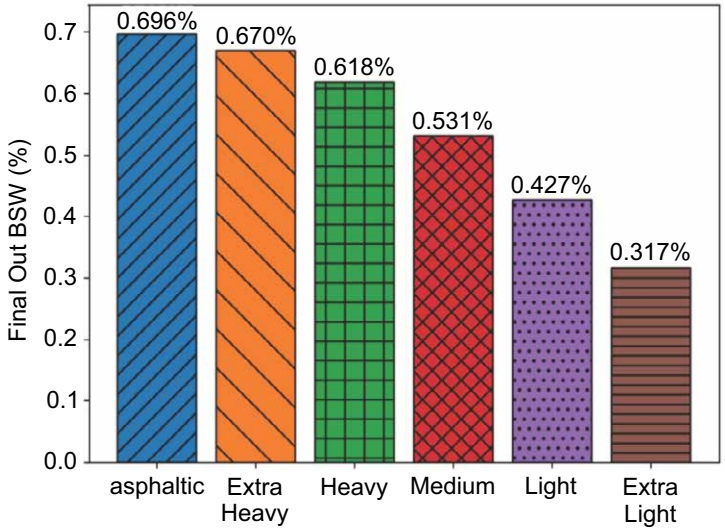

oils with a higher API gravity (lighter) exhibit a lower BS&W content after treatment. This result is a direct consequence of the greater density difference between the oil and water, which facilitates the settling of droplets and results in a more efficient phase separation. Heavier oils have a substantial heavier compound, including naphthenic, asphaltene and paraffinic compound, which help stabilize the emulsions. Thus, the API gravity has an inverse correlation with the BS&W content, and a direct correlation with the separation efficiency. In other words, higher API gravities tend to have better separations.

Conversely, vessel pressure is not significantly affected by variations in oil composition. The model's governing equations ensure a consistent mass balance, where the total liquid outflow is merely partitioned differently between the outlets. For instance, in crudes with a higher BS&W content, a greater volume of entrained water exits with the oil phase, which is offset by a corresponding reduction in flow from the water outlet, as depicted in Figure 8. This redistribution of liquid flow has a negligible impact on the vessel's pressure control loop.

Furthermore, the dynamic response of higher API gravity oils reveals a distinct inflection point

at approximately t = 200 seconds (Figure 8). It is crucial to note that this point represents the peak rate of change during the startup transient, not the onset of stability. Physically, it marks the instant of maximum flow acceleration, after which the system's response begins to dampen as it asymptotically approaches steady-state conditions.

Stabilization of the separator interface levels is preceded by a transient regime, dictated by the primary separation chamber's filling time. Initially, the oil chamber's outflow, without the corresponding supply, generates a negative mass balance, resulting in a decrease in its level. The inflection point occurs when the interface in the primary chamber reaches the 2.8 m mark, corresponding to the spillway, initiating overflow. With the oil chamber's supply restored, the system evolves to a state of equilibrium, in which the interface levels stabilize, as shown in Figures 9-11.

Conclusion

The present work proposed a simulation with different classifications of oils according to the API gravity for the modeling and simulation of a water-oil separation system, which is a three- phase separator. Thus, the current study demonstrated that higher API gravities reduce the BS&W content at the oil outlet, being inversely proportional,

Figure 8. Water outflow by oil gravity.

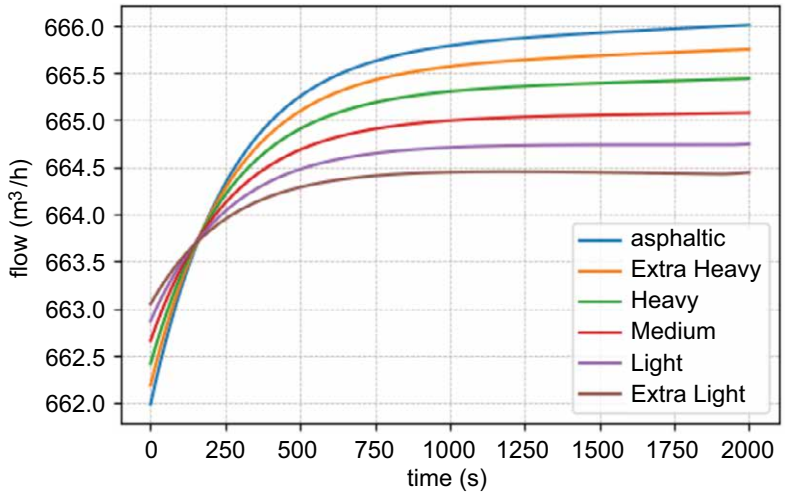

Figure 9. Oil level in separator chamber by oil gravity.

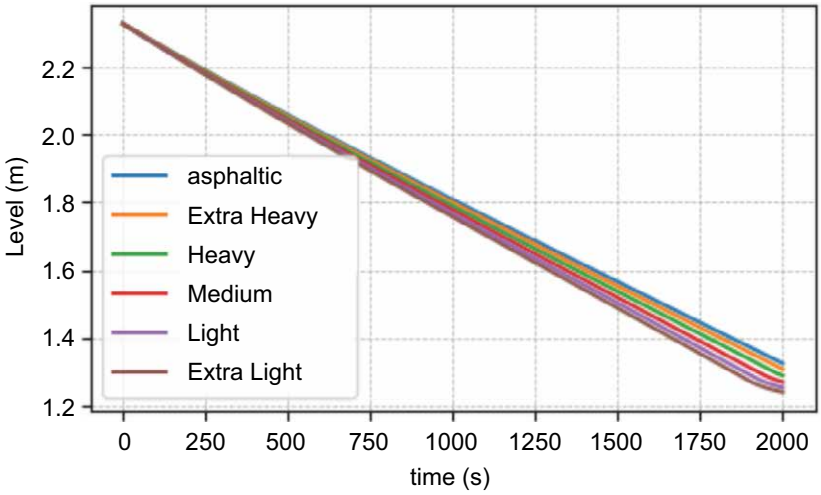

Figure 10. Water level in chamber separator by oil gravity.

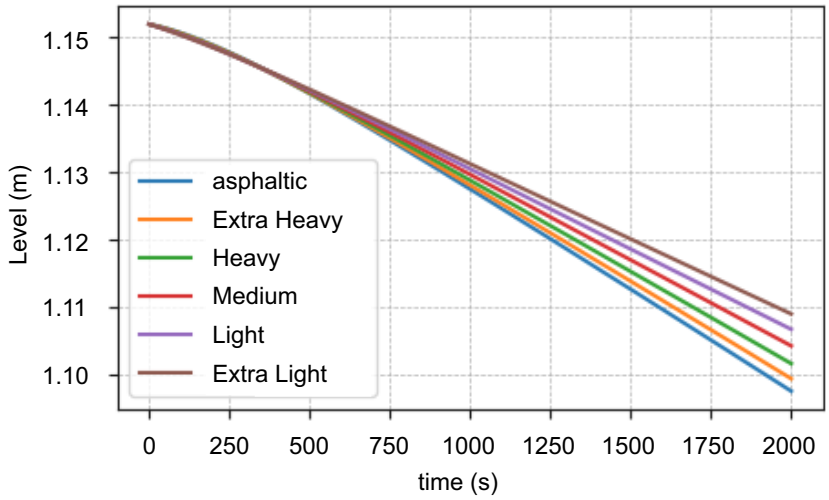

Figure 11. Total Level in chamber separator by oil gravity.

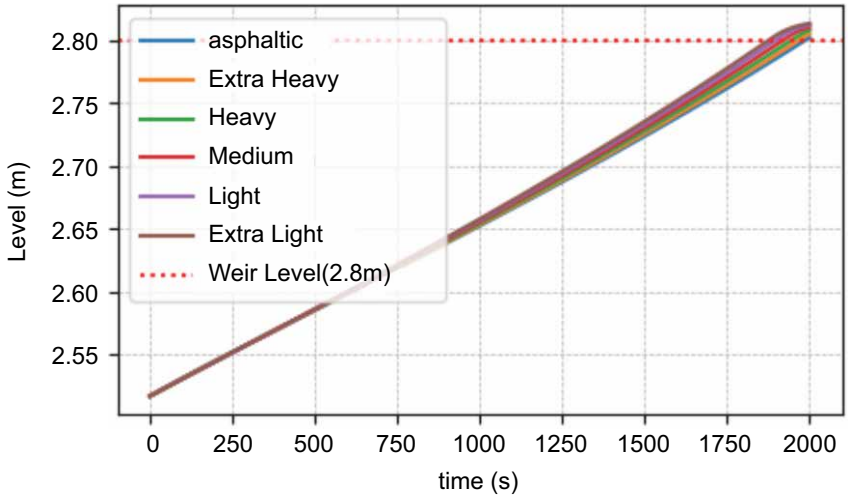

as well as the API gravity does not significantly affect the outlet pressure in the different scenarios, following a trend, as well as the water and total levels in the separation chamber, and oil in the separation chamber.

In summary, the approach to modeling the three- phase separator in Python language presented interesting robustness for applications in different scenarios. For future work, it is recommended to include the implementation of a controller in the percentage of opening of the outlet valves better represents the dynamic system, as well as droplet dynamics, and emulsion thermodynamics, in addition to the experimental validation of the results.

Nomenclature

hwy: Water interface level (m); hly: Oil interface level (m); hty: Total emulsion level (m); hvert: Weir height (m); We, Le,Ge: Inlet water, oil, and gas flow rates (m^3/h); Wsy ,Lsy,Gsy: Outlet water, oil, and gas flow rates (m^3/h); Lvy: Oil flow rate over the weir (m^3/h); Py: Separator pressure (kgf/cm^2); Ty: Temperature (K); Dy: Separator diameter (m); BSWey: Inlet oil BS&W fraction (dimensionless); efwly, eflwy: Separation efficiencies (dimensionless); Sgy,Sly,Swy: Outlet valve openings (%); CVmax: Maximum valve flow coefficient; k: Weir overflow constant

(dimensionless); Ccsy,Ccly: Characteristic length coefficients of the chambers (m); ρfl,ρfw: Density of oil and water (kg/m³).

Acknowledgement

The authors acknowledge the financial support of the Human Resources Program of the National Agency of Petroleum, Natural Gas and Biofuels (PRH/ANP – PRH27.1/SENAI CIMATEC), supported with resources from the investment of oil companies qualified in the RD&I Clause of ANP Resolution No. 50/2015 and the São Paulo Research Foundation (FAPESP), Process No. 2024/12067-7.

References

1. Noik C, Muller S, Karnitz O, et al. subsea separation behavior of a brazilian crude oil. Rio de Janeiro: OTC; 2015. doi:10.4043/26069-MS.
2. Delgado B. síntese de sistemas de regeneração e tratamento final de efluentes [tese]. Rio de Janeiro: Universidade Federal do Rio de Janeiro; 2008. Silvino PFG. análise do grau de agregação do asfalteno e da formação de emulsão água/óleo através de modelo coarse grain [tese]. Fortaleza: Universidade Federal do Ceará; 2018.
3. De Oliveira G. utilização de adsorventes (carvão ativado e argilas organofílicas) no processo de separação de emulsões óleo/água [dissertação]. Campina Grande: Universidade Federal de Campina Grande; 2012.
4. Natividade MC, Campos IOF, Mirre RC. análise comparativa da simulação computacional do processo de separação trifásica de petróleo. In: anais do X SAPCT. Salvador (BA): Doity; 2025.
5. Condori MEG. modelagem matemática e simulação de uma unidade de processamento primário de petróleo no peru [dissertação]. Belo Horizonte: Universidade Federal de Minas Gerais; 2014.
6. Filgueiras NGT. modelagem, análise e controle de um processo de separação óleo/água [dissertação]. Rio de Janeiro: Universidade Federal do Rio de Janeiro; 2005.
7. Natividade M, Campos IOF, Mirre RC. proposta de metodologia para síntese de sistemas de separação de água em óleo visando redução de BSW. In: anais do IX SAPCT. Salvador (BA): Doity; 2024.
8. Junior AMV, Altoé L, Antunes PASBM, et al. principais métodos de tratamento da água produzida em unidades marítimas de produção de petróleo. Lat Am J Energy Res. 2023;10:23-32. doi:10.21712/lajer.2023.v10.n1.p23-32.
9. Nunes GC. modelagem e simulação dinâmica de separador trifásico água-óleo-gás [dissertação]. Rio de Janeiro: Universidade Federal do Rio de Janeiro; 1994.
10. Ribeiro CHP, Miyoshi SC, Secchi AR, et al. model predictive control with quality requirements on petroleum production platforms. J Pet Sci Eng. 2016;137:10-21. doi:10.1016/j.petrol.2015.11.004.
11. Farah MA. petróleo e seus derivados: definição, constituição, aplicação, especificações, características de qualidade. 1ª ed. Rio de Janeiro: LTC; 2012. Burden R, Faires D. numerical analysis. 9th ed. Boston: Richard Stratton; 2010.